

# Melt Processing of Cellulose Acetate for Controlled Release Applications – A Review

Thabang N. Mphateng,\* António Benjamim Mapossa,\* Teboho Mokhena, Suprakas Sinha Ray, and Uttandaraman Sundararaj

Cellulose acetate (CA) has garnered considerable industrial and research interest due to its sustainable properties, such as biodegradability and biocompatibility. Despite these attractive properties, CA is difficult to process using traditional melt processing techniques. This is due to its high crystallinity and a glass transition temperature that exceeds the thermal degradation temperature. Therefore, different additives have been explored to overcome these issues. This review explores recent trends in the use of melt-processed CA materials for encapsulating and controlling the release of active compounds. It highlights the advancements made over the past decade in processing CA-based materials using thermoplastic techniques. Additionally, the review discusses the properties of these materials, including biodegradation, photodegradation, and solubility, which are important for delivering active agents. Finally, it provides an overview of the challenges and prospects for CA-based materials processed through thermoplastic processing methods.

## 1. Introduction

Over the past decades, the use of natural resource-based materials and their composites in various fields, such as catalysis, surface coating, enzyme immobilization, drug delivery, wound dressing, and tissue engineering, has driven significant research and industrial interest.<sup>[1]</sup> These materials are valued

for their ‘green credentials’, such as biocompatibility, biodegradability, and low immunogenicity.<sup>[1]</sup> In this context, cellulose and cellulose-based materials have gained significant attention in both industrial and research sectors because of their abundance and sustainable properties. Amongst these materials, cellulose acetate, a derivative of cellulose, has found widespread use in applications such as cigarette filters, biomedical films and fibers, pollutant adsorbents, and separation membranes.<sup>[2,3]</sup>

The properties of cellulose acetate vary widely depending on the degree of substitution (DS).<sup>[1–3]</sup> The degree of substitution significantly affects the solubility of CA in organic solvents and its melt behavior. The solubility and melt behavior are crucial for the processability of CA.<sup>[4–6]</sup> For instance, CA polymers with a DS between 2.0 and 2.7 are usually used for thermoplastics and are

often processable using different processing techniques. CA materials are typically characterized by high modulus and flexural and tensile strengths. In addition, it can be grafted with other functionalities such as  $-\text{COOH}$ ,  $-\text{SO}_3\text{H}$ , and  $-\text{NH}_2$  to broaden its application.<sup>[1]</sup>

T. N. Mphateng, A. B. Mapossa  
Institute of Applied Materials  
Department of Chemical Engineering  
University of Pretoria  
Lynnwood Road, Pretoria 0002, South Africa  
E-mail: [tnmphateng@sun.ac.za](mailto:tnmphateng@sun.ac.za); [antonio.mapossa@ucalgary.ca](mailto:antonio.mapossa@ucalgary.ca)  
T. N. Mphateng  
Department of Chemistry and Polymer Science  
Stellenbosch University  
Private Bag XI, Matieland 7602, South Africa

A. B. Mapossa, U. Sundararaj  
Department of Chemical and Petroleum Engineering  
University of Calgary  
2500 University Drive NW, Calgary AB T2N 1N4, Canada  
T. Mokhena  
DSI/Mintek Nanotechnology Innovation Centre  
Randburg 2194, South Africa  
S. S. Ray  
Centre for Nanostructures and Advanced Materials  
DSI-CSIR Nanotechnology Innovation Centre  
Council for Scientific and Industrial Research  
Pretoria 0001, South Africa  
S. S. Ray  
Department of Chemical Sciences  
University of Johannesburg  
Doornfontein, Johannesburg 2028, South Africa

 The ORCID identification number(s) for the author(s) of this article can be found under <https://doi.org/10.1002/mame.202500117>

© 2025 The Author(s). Macromolecular Materials and Engineering published by Wiley-VCH GmbH. This is an open access article under the terms of the [Creative Commons Attribution](https://creativecommons.org/licenses/by/4.0/) License, which permits use, distribution and reproduction in any medium, provided the original work is properly cited.

DOI: 10.1002/mame.202500117

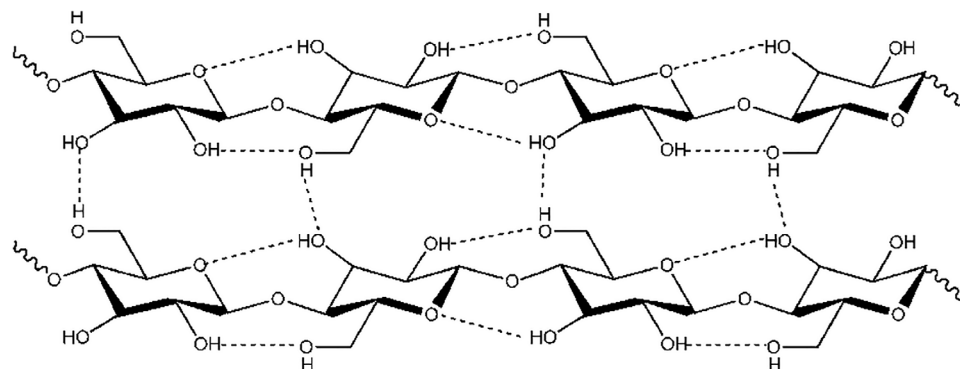


**Figure 1.** Structure of cellulose, with inter- and intramolecular hydrogen bonding.<sup>[19]</sup> Reused with permission from the RSC Publishing.

The exploitation of multifunctional CA materials in various shapes and sizes is a compelling proposition.<sup>[7]</sup> Thermoplastic processing stands out as the most desirable production method, enabling the conversion of solid materials into desired forms. This method is preferred in industrial production because it can blend polymeric materials with various additives or fillers at high temperatures, creating uniform mixtures suitable for various applications.<sup>[7]</sup> The main challenges associated with the melt processing of cellulose acetate (CA) include high viscosity, high glass transition temperature, high crystallinity, and melt processing temperatures that are close to its decomposition temperature. Therefore, modifying CA is crucial not only to improve its processability but also to broaden its applicability. Adding various additives such as plasticizers,<sup>[8]</sup> other polymers,<sup>[9]</sup> and fillers has been considered a suitable solution to overcome these challenges. Literature sources have reported that the use of plasticizers, such as triethyl citrate, glycerol derivatives, and phthalates, improved the processability of CA.<sup>[8,10]</sup> The type and content of the plasticizer play a significant role in the resultant thermal and mechanical performance of CA.<sup>[10–13]</sup> Recent studies have demonstrated that ionic liquids can enhance the processability of CA due to their strong interaction with CA. Bendaoud and Chalame reported that the ionic liquid 1-butyl-3-methylimidazolium chloride (BMIMCl) interacts strongly with CA molecules via van der Waals interactions and hydrogen bonding, weakening CA chain interactions and suppressing crystallinity.<sup>[11]</sup> This results in improved processability of CA at 150 °C, leading to homogeneous and transparent membranes.

Few review papers have investigated the melt processing of cellulose acetate.<sup>[7,14]</sup> To the best of our knowledge, there is no review article that specifically examined the use of melt processing of CA for encapsulation and release technology of active substances. Therefore, this review examines recent trends in the exploration and utilization of melt-processed CA materials for encapsulating and controlling the release of active compounds. It highlights the progress made over the past decade in processing cellulose acetate-based materials using thermoplastic techniques. The review also discusses the properties of these materials, such as biodegradation, photodegradation, and solubility, which are relevant for delivering active agents. Finally, it concludes with an overview of the challenges and future outlook for CA-based materials processed through thermoplastic methods.

## 2. Preparation and Properties of Cellulose Acetate

Cellulose is the most abundant natural polymer and is usually obtained from the *Eucalyptus* species as a major commercial source.<sup>[15,16]</sup> It is a homopolymer of glucose, with the monomers connected by  $\beta$ -1,4 glycosidic linkages. Cellulose is arranged in microfibrils, which make up plant cell walls, thus making it a significant structural feature in plants. Therefore, it has great stability and mechanical properties.<sup>[17]</sup> The stability of cellulose results from the strong intramolecular and intermolecular hydrogen bonding (**Figure 1**), resulting in high crystallinity. This, unfortunately, results in a glass transition temperature that exceeds the thermal decomposition temperature,<sup>[2,18]</sup> which makes it difficult to process cellulose using conventional polymer processing techniques, such as melt extrusion and injection molding. In addition, cellulose is also insoluble in common organic solvents. To address this problem, cellulose has been derivatized via esterification to yield thermoplastic polymers, such as cellulose acetate, cellulose acetate butyrate cellulose acetate propionate, cellulose nitrate, and carboxymethyl cellulose, which feature modified thermal properties that allow thermal processing by melt extrusion.<sup>[18]</sup>

Cellulose acetate is one of the most popular cellulose derivatives (**Figure 2**). The derivatization to cellulose acetate is achieved through the following processes: the methylene chloride process, the heterogeneous process, and the acetic acid process. The commonly used derivatization process for the production of cellulose

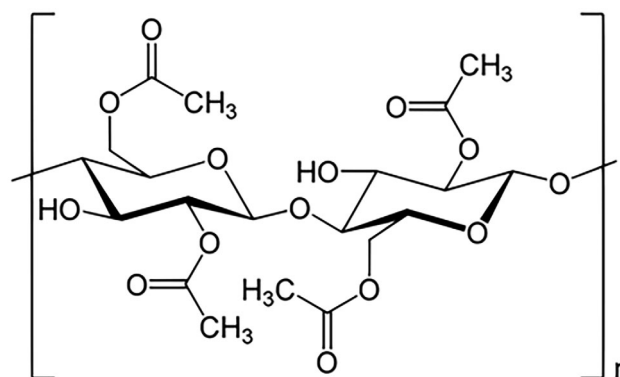


**Figure 2.** Molecular structure of cellulose acetate (DS $\approx$ 2).

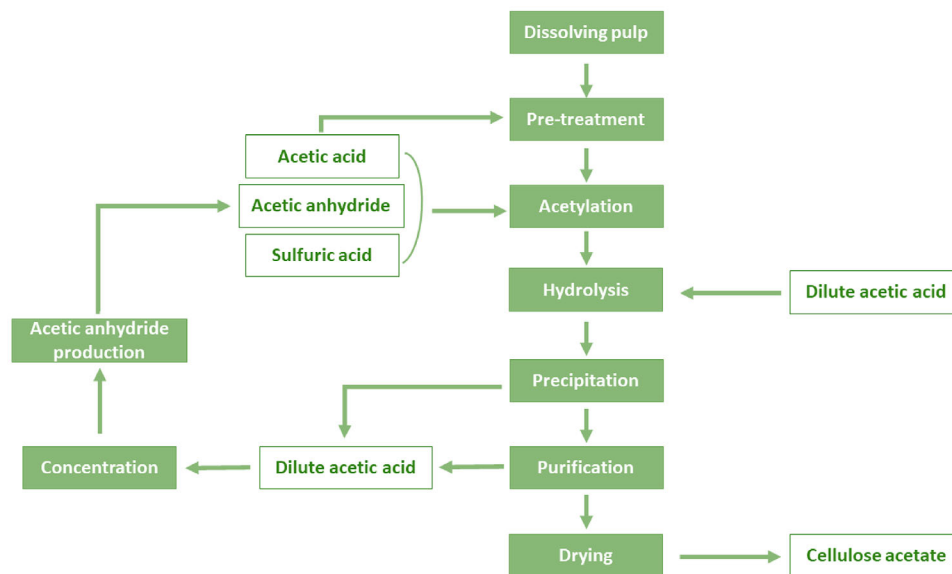


**Figure 3.** Simplified process flow diagram for the industrial production of CA from cellulose. Adapted from Bao (2015).

acetate on an industrial scale is the acetic acid process, shown in **Figure 3**, which occurs by esterification with acetic anhydride.<sup>[5]</sup> In the presence of a sulphuric acid catalyst, the acetyl group from the acetic anhydride undergoes a substitution reaction with the hydroxyl groups of cellulose to produce cellulose acetate (see **Figure 2**). Initially, a trisubstituted cellulose acetate (cellulose triacetate) is produced. Thereafter, the degree of substitution can be tailored by the hydrolysis of acetyl substituents with water and dilute acetic acid to produce mono- or di-substituted cellulose diacetate.<sup>[5,20]</sup>

The properties and, by extension, applications of cellulose acetate are significantly influenced by the DS, which is the average number of substituent acetyl groups per anhydroglucose ( $\beta$ -glucopyranose) unit.<sup>[4,5]</sup> Cellulose diacetate (DS between 2.0 and 2.7) is a semi-crystalline and biodegradable thermoplastic polymer, whereas cellulose triacetate (DS  $\geq 2.9$  features a higher degree of crystallinity and is easier to melt process, but less biodegradable.<sup>[10,15,21]</sup> In contrast to cellulose, CA is soluble in common organic solvents and much less crystalline.<sup>[4]</sup> However, it is brittle and stiff, which limits its applications. Therefore, external plasticization is necessary in order to turn it into a useful thermoplastic material.<sup>[22]</sup> The addition of low molecular weight plasticizers significantly reduces the glass transition temperature ( $T_g$ ), improving material flexibility and toughness.<sup>[23]</sup> In addition, it reduces the melt viscosity, which also extends the thermal processing window to lower temperatures, resulting in much easier processing.<sup>[3,10,16,22]</sup>

### 3. Bio- and Photodegradation of Cellulose Acetate

Cellulose is widely known to be biodegradable and is readily degraded by organisms that have the cellulase enzyme. CA, due to the presence of acetyl groups, requires an additional enzyme to undergo full biodegradation. Firstly, CA must undergo deacetylation, whereby acetyl esterase enzymes break down the ester bonds by hydrolysis, leaving the cellulose backbone. The remain-

ing cellulose backbone is completely degraded by a three-enzyme system consisting of  $\text{exo-}\beta$ -1,4-glucanase,  $\text{endo-}\beta$ -1,4-glucanase, and  $\beta$ -glucosidase in microorganisms, such as bacteria, fungi, and algae; thus completing the biodegradation process, as shown by **Table 1**.<sup>[15,24]</sup> Since cellulose triacetate (CTA) has more acetyl groups than cellulose diacetate, it would require more enzymatic activity and energy for the hydrolysis reaction.

Furthermore, the hydrolysis of cellulose triacetate is more stable than that of cellulose diacetate due to the higher moisture absorption of the diacetate polymer.<sup>[25]</sup> Therefore, CA polymers with a lower DS have more potential for biodegradation, whereas a high DS (2-3) value means more acetyl groups that disrupt the ordered structure of cellulose.<sup>[4,26,27]</sup> This is supported by the studies conducted by Buchanan et al.<sup>[28]</sup> on the biodegradability of cellulose acetate with respect to the degrees of substitution. According to their findings, biodegradation rates were greatly reduced, but not inhibited, by the higher levels of acetyl (higher DS). This implies that the rate of biodegradability of CA is reduced when the degree of substitution is increased, thus making cellulose triacetate less biodegradable than cellulose diacetate. Furthermore, cellulose diacetate is usually biodegradable when the DS does not exceed 1.5.<sup>[18,26]</sup>

Biodegradation depends on a combination of natural factors, such as soil composition, presence of microorganisms, and moisture content. Additionally, Puls et al.<sup>[15]</sup> reported that successful biodegradation of biopolymers is dependent on factors such as temperature, pH, and oxygen concentration, in the environment in which the biopolymer is to be subjected. Other factors that may affect the biodegradation of biopolymers include the chemical structure, type of biopolymer, crystallinity, and chain mobility.<sup>[29]</sup> In aerobic conditions, biopolymers decompose into monomers and shorter oligomer chains, which are ultimately converted to  $\text{CO}_2$ ,  $\text{H}_2\text{O}$ , and cell biomass, whereas methane and hydrogen are by-products in anaerobic conditions. Furthermore, a wide functional and phylogenetic diversity is required in the microbial community for the complete biodegradation of cellulosic

**Table 1.** The chemical reactions involved in the complete biodegradation of cellulose.<sup>[30]</sup>

Reaction	Microbial process	Chemical reaction
1	Hydrolysis of cellulose into $\beta$ -D-cellobiose	Cellulose $\rightarrow$ $\beta$ -D-cellobiose
2	Hydrolysis of $\beta$ -D-cellobiose and fermentation	$\beta$ -D-cellobiose $\rightarrow$ volatile organic acids + CO <sub>2</sub> + H <sub>2</sub>
3	Hydrogenotrophic methanogenesis	4H <sub>2</sub> + CO <sub>2</sub> $\rightarrow$ CH <sub>4</sub> + 2H <sub>2</sub> O
4	Acetogenesis	4H <sub>2</sub> + 2CO <sub>2</sub> $\rightarrow$ CH <sub>3</sub> COOH + 2H <sub>2</sub> O
5	Aceticlastic methanogenesis	CH <sub>3</sub> COOH $\rightarrow$ CH <sub>4</sub> + CO <sub>2</sub>

materials.<sup>[30]</sup> The chemical reactions involved in the biodegradation of CA are shown in Table 1.

A study by Tselana and co-workers investigated the biodegradability of CA (DS 2.4), CA plasticized with polyethylene glycol (PEG400) at 35 wt.%, and its blends with polybutylene adipate-co-terephthalate (PBAT) and polylactic acid (PLA) through CO<sub>2</sub> biodegradation tests conducted in a respirometric biodegradation flask system, using the standard ASTM D5338 test method.<sup>[31]</sup> The total degradation was measured by the total CO<sub>2</sub> emitted from the flask system based on the total organic carbon present in the initial test sample. Their results, presented in Figure 4, showed good biodegradability of neat cellulose and CA over a period of 100 days. However, the plasticization with PEG significantly reduced the overall biodegradation rate. This was then improved by blending with PLA and PBAT. In another study, Phuong et al.<sup>[3]</sup> conducted CA biodegradation tests according to the ISO 14855-1 (2012) international standard, and the evolution of CO<sub>2</sub> was tracked as an indicator for biodegradation. They reported that complete biodegradation of CA (DS $\approx$ 2.4) was achieved over a period of 200 days under controlled composting

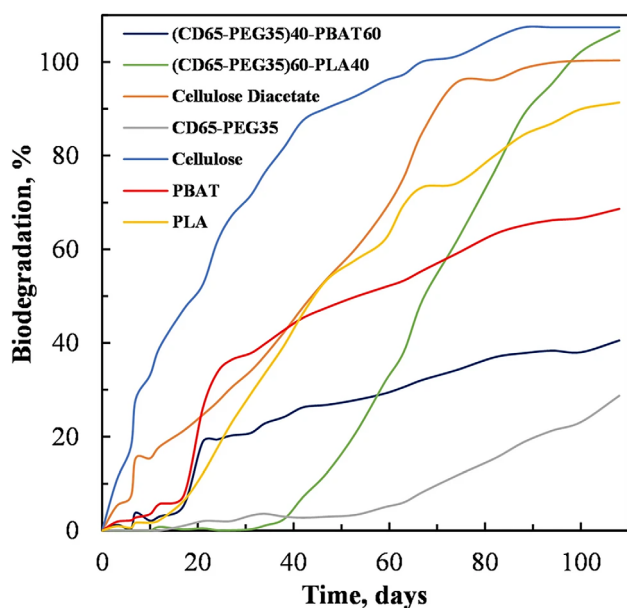


**Figure 4.** Biodegradation profiles of neat cellulose, CA, PLA, and PBAT; CA plasticized with 35 wt.% PEG (CD65-PEG35); and CA-PEG blended with 40 wt.% PLA ((CD65-PEG35)60-PLA40) and PBAT ((CD65-PEG35)40-PBAT60).<sup>[31]</sup> Reproduced under the Creative Commons Attribution 4.0 International License.

conditions, aided by inoculations with biowaste. Furthermore, CA plasticized with triacetin, diacetin, and a 1:1 triacetin-diacetin mixture reached complete biodegradation after 46 days, indicating a significant effect of the plasticizers on the acceleration of biodegradability. This accelerated biodegradation of CA due to the incorporation of plasticizers was also reported by Buchanan et al.<sup>[32]</sup> in a study that entailed the blending of CA (DS $\approx$ 2.5) with CA (DS $\approx$ 2.0) and plasticization with PEG400. In both studies by Tselana et al.<sup>[31]</sup> and Phuong et al.,<sup>[3]</sup> biodegradation percentages exceeded 100% for some of the samples, attributed to the synergistic “priming effect” that occurs when the compost inoculum in the samples produces more CO<sub>2</sub> than the compost in the control experiment. This results in a net production of CO<sub>2</sub> that is not exclusively from the test sample, and an overestimation of the biodegradation percentage.<sup>[3,33,34]</sup>

Cellulose acetate absorbs light at a wavelength of  $\approx$ 260 nm, which, according to Puls et al.<sup>[15]</sup> can be attributed to the presence of the carbonyl functional groups in the acetyl substituents. The authors also deduce that cellulose acetate does not significantly undergo photodegradation in the natural environment because radiation from the sun reaches the Earth only at wavelengths exceeding 300 nm. This could be disadvantageous, considering that the material may take longer to degrade due to the high photostability. The addition of titanium oxide<sup>[15]</sup> or benzophenone<sup>[35]</sup> during processing could accelerate the photodegradation of cellulose acetate if such is desired. However, for agricultural and bio-related applications, it is not recommended due to the environmental and health risks associated with these compounds.

## 4. Processability of Cellulose Acetate-Based Materials

### 4.1. Cellulose Acetate

The thermal processability of cellulose acetate depends significantly on its degree of substitution.<sup>[18]</sup> Differential Scanning Calorimetry (DSC) analysis shows that the glass transition temperature ( $T_g$ ) decreases with an increase in the DS (Figure 5a). As a result, the trisubstituted cellulose acetate (DS = 2.95) has a lower glass transition temperature ( $T_g$ ) than other CA grades and is thus relatively easier to process. Dreux et al.<sup>[23]</sup> reported that the melt processing of CA is possible only for a degree of substitution close to 2.5 (cellulose diacetate), which is in contrast with the trend established by Teramoto,<sup>[18]</sup> that melt processability, based on  $T_g$ , becomes easier with a higher DS. It appears that Dreux’s remarks were based on the melting temperature ( $T_m$ ) being slightly below the decomposition temperature ( $T_d$ ) at only DS  $\approx$ 2.5 (Figure 5b), and not on the  $T_g$  (which is the common

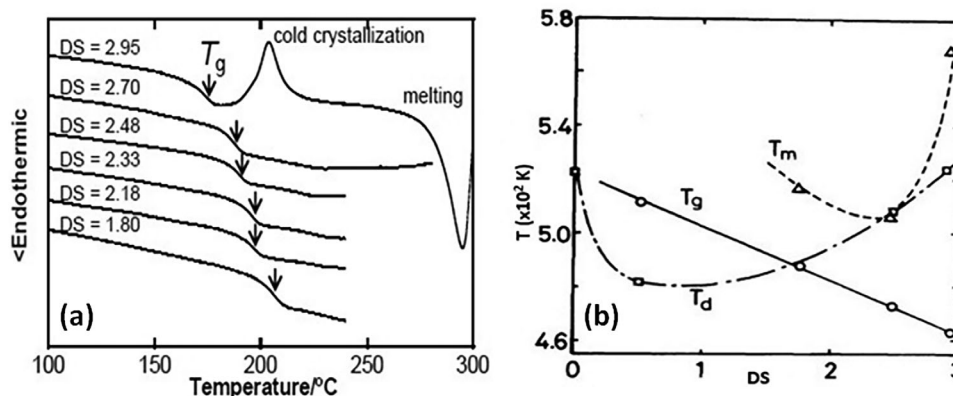


**Figure 5.** a) DSC thermogram showing the effect of DS on the  $T_g$  of CA.<sup>[18]</sup> MDPI. Reused under the Creative Commons Attribution License. b) Illustration of the effect of DS on processing, glass transition, and decomposition temperatures of CA.<sup>[36]</sup> Reused with permission from Springer Nature.

reference parameter for processability) trend presented in the same figure.

## 4.2. Cellulose Acetate-Plasticizer Systems

### 4.2.1. Cellulose Acetate-Plasticizer Systems: Recent Advances

Pure CA consists of strong intra- and intermolecular hydrogen bonding between its free hydroxyl groups and the carbonyl ester groups, resulting in a high  $T_g$ , which is also close to, and in some cases, above its thermal decomposition temperature, depending on the DS (Figure 5). This makes conventional melt processing of CA difficult without the use of plasticizers or blending with other polymers. However, blending CA with other polymers is also difficult due to the high polarity of CA. For example, blends of CA/CA-propionate and CA/CA-butyrate are immiscible despite their similar molecular structures.<sup>[22]</sup>

CA is highly hydrophilic, which leads to high moisture absorption.<sup>[3,37]</sup> Therefore, before processing by extrusion compounding and injection molding, CA needs to be vacuum/oven

dried to prevent hydrolytic degradation.<sup>[37]</sup> The polymer can be dried for at least 24 h at temperatures between 70 °C<sup>[23,38,39]</sup> and 80 °C.<sup>[40]</sup> Thereafter, CA can be processed within a temperature profile of 170–200 °C.<sup>[22,38,41–43]</sup> However, this can only be achieved through the use of external plasticizers such as triacetin, triethyl citrate, and diethyl phthalate.<sup>[5]</sup> Plasticizers often enter into the amorphous parts of a polymer, while the structure and size of the crystalline parts remain unaffected. However, the crystalline structure can collapse as the plasticizer content increases, as depicted in Figure 6.<sup>[39]</sup> Moreover, plasticizers generally reduce the melt viscosity, glass transition temperature, and volume resistivity of a polymer, while increasing its free volume. This results in reduced interactions between polymer chains due to the shielding of polar functional groups,<sup>[22]</sup> thus increasing molecular mobility and ease of processing.<sup>[5]</sup> An ideal plasticizer must be compatible with CA at an appreciable amount, depending on the degree of substitution. Furthermore, it must be retained in the matrix for an acceptable aging period without inducing acidity.<sup>[44]</sup> and be stable in any kind of temperature environment.<sup>[5]</sup> As a result, plasticizers with a significantly low water solubility are recommended because they

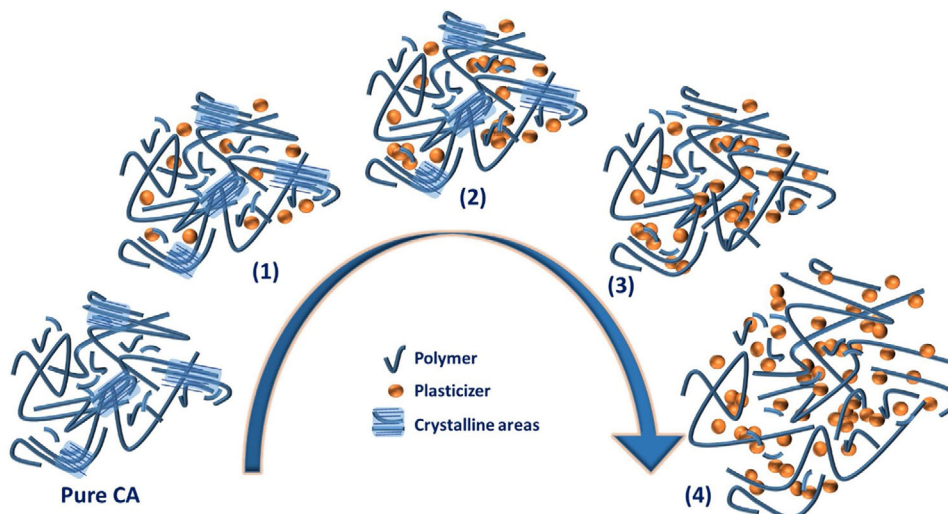


**Figure 6.** Illustration of the effect of plasticizer content on the chain structure of CA.<sup>[39]</sup> Reused with permission from Elsevier.

**Table 2.** Selected studies on the thermoplastic processing of CA-based materials.

Formulation	DS	Pre-processing	Processing	Post-processing	Verdict	Refs.
CA/diethyl phthalate (DEP)	2.5 <sup>a)</sup>	–	Melt compounding at 150 rpm and 150 °C for	Melt-pressed at 150 °C and 200 bar for 10 min	The resultant samples were clear and transparent, homogeneous, and flexible when using DEP but BMIMCl led to transparent, flexible, and colored samples. Therefore, BMIMCl ionic liquid can be used as a green and safe plasticizer	[11]
CA/oleic acid (OLA)	2.4–2.5 <sup>a)</sup>	Solution casting	Extruded at 45 rpm and 80 °C	–	Oleic acid serves as a good plasticizer because of the oleate groups act as internal plasticizers	[47]
CA/nanofiller	2.5 <sup>a)</sup>	Melt mixer 230 °C, 100 rpm for 8 min	Extruded at temperatures between 130 and 240 °C	–	Functionalization of the nanofillers and extrusion partially improved the dispersion	[48]
CA/starch	2.5 <sup>a)</sup>	–	Extruded at temperatures between 90 and 120 °C	Melt-pressed at 130 °C and 50 bar for 10 min	The as-prepared films exhibited good shape-memory features	[49]
CA/PEG/PBAT & CA/PEG/PLA	2.4	Mechanical premixing	Extruded at temperatures between 120–160 °C, and 40–45 rpm	Injection moulded: temperature profile between 180–200 °C, 95 bar for 60s an demolding temperature 25–35 °C	The presence of plasticizers improved the overall processability	[31]

<sup>a)</sup> DS calculated from acetyl content (%) as per the method proposed by Fei et al.<sup>[4]</sup>

reduce the risk of moisture absorption.<sup>[44]</sup> Moreover, a plasticizer with high moisture absorption tends to leach out of CA, which results in brittleness, leading to rapid aging and degradation of the material.<sup>[44]</sup>

Plasticizers, such as dimethyl phthalate (DMP) and diethyl phthalate (DEP), have been under scrutiny due to environmental and health concerns. As a result, there has been a significant rise in the melt-processing of CA with environmentally benign plasticizers, such as glycerol derivatives, citrate esters, and polyethylene glycols.<sup>[8,45,46]</sup> It is worth mentioning that there is a minimum and maximum content of the plasticizer at which CA can be melt processed. For instance, Bendaoud and Chalamet reported that CA (DS ≈2.5) was not processable at a plasticizer content below 20 wt%.<sup>[11]</sup> However, when exceeding 40 wt.%, the mechanical performance of the resultant materials was negatively affected. Depending on the surface functionalities of the plasticizer, there can be good interaction with the CA.<sup>[47]</sup> Tedeschi et al.<sup>[47]</sup> studied the esterification of CA (DS 2.4–2.5) using oleic acid (OLA). Oleic acid was found to be compatible with CA, leading to more hydrophobic materials and good water vapor barrier properties. The resultant materials were flexible due to the available oleate groups acting as internal plasticizers with the CA chains. Other studies on the processing of CA with various plasticizers are summarized in **Table 2**.

#### 4.2.2. Applying Solubility Parameters to Determine Suitable Plasticizers for Cellulose Acetate

The efficiency of a plasticizer depends largely on its compatibility and miscibility with the polymer.<sup>[22]</sup> The compatibility of a polymer and solvent can be predicted using the Hildebrand solubility parameter ( $\delta$ ).<sup>[50]</sup> This is based on a “like dissolves like” concept, whereby compatible polymer-solvent systems would have little enthalpy change upon mixing.<sup>[51–53]</sup> This method is

reasonably accurate when the interactions between the components are purely dispersive,<sup>[51]</sup> applicable in polymer-solvent systems such as polyolefins and nonpolar solvents. However, for systems that incorporate more complex intermolecular interactions, the method becomes insufficient, and Hansen’s approach becomes more useful, as it involves splitting Hildebrand’s solubility parameter into three fundamental intermolecular interactions; dispersion ( $\delta_D$ ), polarity ( $\delta_P$ ) and hydrogen bonding ( $\delta_H$ ) interactions,<sup>[51,54]</sup> expressed by Equation 2 as follows:

$$\delta_T = \sqrt{\delta_D^2 + \delta_P^2 + \delta_H^2} \quad (1)$$

The solubility parameter represents the total cohesive energy density due to the additive effects of these interactions. As such, some solvents may have similar  $\delta_T$ -values and still exhibit different solubility behavior due to the differences in the contributions by the individual interactions.<sup>[55]</sup> Using Hansen’s method, an approximately spherical solubility area can be constructed in a 3D coordinate system, with the axes defined by the individual solubility parameters. The radius of this solubility sphere ( $R_0$ ) is used to predict solubility between the solvent and the polymer,<sup>[56]</sup> and gives the boundary that separates good solvents from poor solvents. Solvents that are contained within the sphere have good compatibility with the polymer, and those outside the sphere are poor solvents.<sup>[57]</sup> This prediction can be made using Equation 3:

$$R_a = \sqrt{4(\delta_{Ds} - \delta_{Dp})^2 + (\delta_{Ps} - \delta_{Pp})^2 + (\delta_{Hs} - \delta_{Hp})^2} \quad (2)$$

whereby  $R_a$  is the distance of the solvent from the center of the polymer solubility sphere, and  $\delta_{Xs}$  and  $\delta_{Xp}$  are the Hansen component parameters for the solvent and polymer, respectively. From the equation,  $R_a < R_0$  suggests good compatibility, whereas poor polymer-solvent compatibility is indicated by  $R_a > R_0$ .<sup>[55,58]</sup>

**Table 3.** Hansen Solubility Parameters and calculated solubility sphere values for cellulose acetate, selected conventional plasticizers, plant-based volatile compounds, and common solvents.

	$\delta_D$ [MPa <sup>1/2</sup> ]	$\delta_P$ [MPa <sup>1/2</sup> ]	$\delta_H$ [MPa <sup>1/2</sup> ]	$\delta_T$ [MPa <sup>1/2</sup> ]	$R_0$ [MPa <sup>1/2</sup> ]	$R_g$ [MPa <sup>1/2</sup> ]	Refs.
CA	14.9	7.1	11.1	19.9	12.4	–	[59, 60]
Triethyl citrate	16.5	4.9	12.0	20.9	–	4.0	[56]
Triacetin	16.5	4.5	9.1	19.4	–	4.6	[61]
PEG200	16.7	5.6	16.7	24.3	–	6.8	[62]
PEG400	14.6	7.5	9.4	18.9	–	10.7	[63]
Linalool	16.3	4.4	11.2	20.3	–	3.9	[64]
Terpineol	13.9	8.0	10.2	19.0	–	2.4	[64]
Camphor	17.3	10.0	4.9	20.6	–	8.4	[64]
Geraniol	16.3	4.1	11.3	20.3	–	4.1	[64]
Methyl salicylate	16.0	8.0	12.3	21.7	–	2.7	[60]
Citronellol	16.1	4.8	10.8	19.9	–	3.3	[64]
1,8-cineole	16.7	4.6	3.4	17.7	–	8.9	[65]
L-Menthol	16.0	4.7	9.0	18.9	–	3.9	[65]
Thymol	19.0	4.5	10.8	22.3	–	8.6	[65]
Acetone	15.5	10.4	7	19.9	–	5.4	[58]
Dichloromethane	18.2	6.3	6.1	20.2	–	8.3	[66]
Methanol	15.1	12.3	22.2	29.5	–	12.3	[66]
Water	15.6	16.0	42.3	47.8	–	32.5	[58]

Hansen's solubility parameters can be used to determine the compatibility of the active compounds with cellulose acetate.<sup>[22]</sup> According to Majumder et al.<sup>[59]</sup> CA can form homogenous solutions with compounds with  $\delta_T$  – values of 19.43–25.57 MPa<sup>1/2</sup>. Furthermore, Ghorani et al.,<sup>[56]</sup> Majumder et al.,<sup>[59]</sup> and Swapnil et al.,<sup>[58]</sup> reported an  $R_0$  value of 12.40 for CA. Therefore, the compatibility of the selected active compounds with CA is then determined by Equations 1 and 2, and the parameters are detailed in Table 3, which shows that the selected active compounds are potentially compatible with CA and could thus function as plasticizers. Moreover, HSP values of nonsolvents such as water (47.8) and methanol (29.5) are also included. Since these fall outside the range specified earlier, they are not expected to be compatible with CA, which verifies the validity of the solubility parameter approach.

### 4.3. Cellulose Acetate-Based Polymer Blends

In some cases, blending CA with other polymeric materials is used not only to enhance thermal processability but also to expand its practical applications.<sup>[49]</sup> Polymer blends are materials that result from mixing at least two distinct polymers, mainly without chemical interactions. These are classified according to their miscibility as completely miscible, partially miscible, and completely immiscible blends.<sup>[31,67]</sup>

Similar to plasticization, blending also relies on miscibility, which enables homogeneity during processing. Miscibility of polymers is also dependent on factors such as temperature and blend composition, i.e., mass fractions of component polymers in the blend.<sup>[68,69]</sup> For instance, completely miscible blends are

characterized by a single  $T_g$  and a homogenous morphology due to lower interfacial tension (approaching zero) between component polymers. Additionally, the  $T_g$  of the blend can be predicted from the mass fractions of the component polymers ( $w_1$  and  $w_2$ ) and their individual  $T_g$  values ( $T_{g,1}$  and  $T_{g,2}$ ) using various equations that have been proposed previously,<sup>[70–73]</sup> with the Fox equation (Equation 3) gaining frequent use due to its simplicity.<sup>[70,74]</sup>

$$\frac{1}{T_g} = \frac{w_1}{T_{g,1}} + \frac{w_2}{T_{g,2}} \quad (3)$$

For partially miscible blends, the  $T_g$  of one component polymer tends to shift toward that of the second component, whereas immiscible blends are characterized by two distinct  $T_g$  values, in addition to poor interfacial interactions between component polymers, leading to a heterogenous morphology and poor mechanical properties. These are typically characterized using techniques such as differential scanning calorimetry (DSC), dynamic mechanical analysis (DMA), thermogravimetric analysis (TGA), tensile testing, and scanning electron microscopy (SEM).<sup>[67,75,76]</sup>

Tselana et al.<sup>[31]</sup> prepared CA-based blends with a plasticizing agent, polyethylene glycol (PEG). In their work, PEG-plasticized CA was blended with poly(lactic acid) (PLA) and poly(butylene adipate-co-terephthalate) (PBAT) via melt extrusion and injection molding. It was reported that PEG reduced the glass transition temperature ( $T_g$ ) from 220 °C to 100 °C, thereby improving processability. The optimal content of 35 wt.% CA plasticized with PEG was found to enhance the melt processing of the blends.

In another study, plasticized CA (pCA) was blended with thermoplastic starch (TPS) and PBAT (pCA-TPS and pCA-TPS-PBAT) by extrusion at 180 °C and 200 °C, depending on the formulations.<sup>[76]</sup> The authors demonstrated that blending the polymers at higher temperatures (200 °C) resulted in more homogeneous blends with superior mechanical properties. Moreover, pCA-TPS blends were characterized by superior tensile strength, Young's modulus, and elongation-at-break at 75:25 and 50:50 pCA-TPS ratios at both processing temperatures. However, pCA-TPS-PBAT blends exhibited poor mechanical properties and overall inhomogeneity despite compatibility between pCA and TPS. This was attributed to competitive pCA-TPS and PBAT-TPS interactions, whereby two components interacted strongly and isolated the third component.

Meereboer et al.<sup>[77]</sup> blended triethyl citrate (TEC)-plasticized CA (pCA) with poly(3-hydroxybutyrate-co-3-hydroxyvalerate) (PHBV) by extrusion and injection molding. Their work demonstrated the polymer blends are immiscible at all investigated blend ratios, despite predictions of miscibility by solubility parameters. Mechanical testing results showed that the PHBV/pCA (30:70) blends had the highest impact strength compared to both individual PHBV and pCA components. However, the blends also exhibited low elongation-at-break (less than 2.5 %), at all blend ratios, which was much lower than that of pCA. These were attributed to the degradation of PHBV at high processing temperatures (200–210 °C), which also resulted in lower tensile and flexural strengths for the blends compared to the component materials.

Marques and coworkers blended CA with zein in a 60:40 weight ratio by solution casting.<sup>[78]</sup> Incorporated in the blend were glycerol (G) and tributyrin (T) as plasticizers, added at 30 wt.% relative to the blend, and 10 wt.% garlic essential oil (GEO), for potential application in active food packaging. The blends exhibited underwhelming performance compared to control films made of CA-T and CA-T-GEO in terms of tensile strength, elongation-at-break, and young's modulus. Moreover, the blends also had higher water vapor permeability than the control films, thus negatively impacting their feasibility for the intended application. The authors justified this by highlighting the effect of the additivity rule, whereby the properties of the blends reflected average properties of component polymers, with no synergism or incompatibility observed.

These studies show that miscibility is still a great challenge in CA-based blends compared to CA-plasticizer systems. Furthermore, most polymer blends have been found to be thermodynamically immiscible; necessitating continued research efforts on understanding the architecture of polymer blends and optimizing miscibility.<sup>[67]</sup> This is particularly important for CA-blends, given its complexity and lack of miscibility with other polymers.

#### 4.4. Cellulose Acetate-Clay Nanocomposites

In the past few decades, nanofillers (particles that have at least 1D in the nanometre scale) have gained traction as additives in polymer processing. Such fillers can include inorganic and organo-modified clays, silica (SiO<sub>2</sub>) nanoparticles,

carbon nanotubes, graphene, starch nanocrystals, cellulose-based nanofibers (CNFs), nanocrystals (CNCs) and nanowhiskers (CNWs), chitin/chitosan nanoparticles and other inorganic materials.<sup>[79–81]</sup> These result in polymeric materials typically characterized by improved barrier properties (lower gas and liquid permeabilities), improved tensile strength, and tensile modulus without significantly compromising the impact strength.<sup>[41,82]</sup> This review will focus on clay nanofillers and their effects on the properties and applications of melt-processed CA because of their easy accessibility and cost-effectiveness.

MMT clays (**Figure 7**) are the most common and effective nanofillers in polymer-clay nanocomposite materials (including CA-based materials). This is mainly due to their abundance, low cost, large surface area, and high cation-exchange capacity. As a result of their high cation exchange capacity, the Na<sup>+</sup>, K<sup>+</sup>, and Ca<sup>2+</sup> cations in the interlayer space can be replaced with organic cations such as alkylammonium, phosphonium, and sulfonium ions to make the clay compatible with non-polar polymers.<sup>[83–86]</sup> The ease of modification of the clay results from the weak electrostatic forces that hold the layered nanoplatelets, which makes it easier for the interlayer space to be penetrated by organic cations, polar organic liquids, and water, resulting in the expansion of the lattice (**Figure 8**).<sup>[84]</sup> The organic surfactants are known to increase the interlayer spacing, which improves polymer-clay compatibility, since the polymer chains are able to penetrate the interlayer spacing, thus improving the clay dispersion within composites. As a result, good clay dispersion is obtained for nanocomposites prepared with organoclays.<sup>[87–89]</sup>

The preparation of clay-based polymer nanocomposite materials by melt-processing has great advantages because it is environmentally friendly, due to the absence of organic solvents. Furthermore, it is also compatible with conventional industrial polymer processing methods such as extrusion compounding and injection molding.<sup>[90]</sup> Importantly, layered clay silicates are sufficiently compatible with polymers under molten (processing) conditions.

The polymer matrix can form phase-separated microcomposites or intercalated nanocomposites, which are characterized by the moderate infusion of polymer chains into the nanoplatelets while retaining the layered structure of the filler. With further shearing, the layered structure is dissipated, and individual platelets are further dispersed into the polymer matrix to form exfoliated nanocomposites (**Figure 9**). The formation of phase-separated composites occurs when the polymer is unable to intercalate between the nanofiller sheets/layers, and the resulting properties stay in the same range as those of traditional microcomposites.<sup>[79,80,91]</sup> Furthermore, clay tactoids are formed throughout the matrix, and no separation of clay nanoplatelets occurs, resulting in micron-sized agglomerates.<sup>[83]</sup>

Characterization techniques for the morphology of polymer nanocomposites (PNCs) include X-ray diffraction (XRD) and transmission electron microscopy.<sup>[88–90,93,94]</sup> Due to its availability and convenience, XRD is the most commonly used technique for studying PNC morphology.<sup>[90]</sup> However, it is only limited to the characterization of intercalated nanocomposites due to their well-ordered and preserved multilayer morphology. This allows the interlayer spacing to be determined using Bragg's law. For exfoliated nanocomposites, no diffraction peaks are

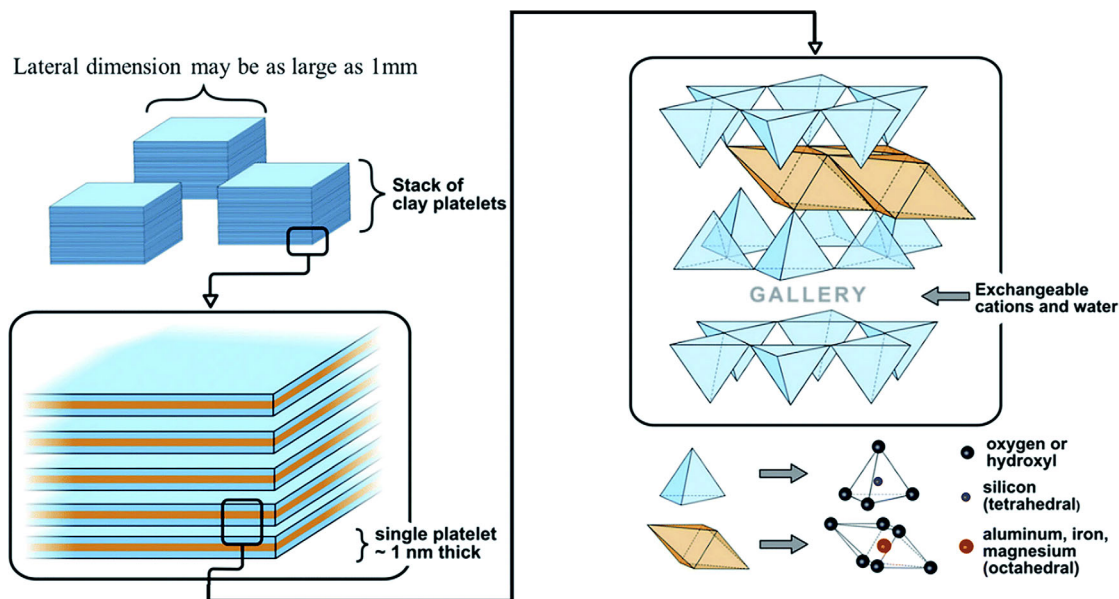


Figure 7. Structure of layered silicate MMT clay.<sup>[83]</sup> Reused with permission from RSC Publishing.

visible in the diffractograms for two possible reasons: (i) too much spacing between the nanofiller layers, (ii) random dispersion of nanofiller layers, which does not present any consistency in the ordering of the particles (Figure 10). Therefore, TEM becomes more useful for characterizing the morphology of exfoliated nanocomposites.<sup>[79]</sup>

CA polymers, similar to most bio-based polymers, have poor thermal and mechanical properties<sup>[96]</sup> and low chemical resistance<sup>[97]</sup> when compared to petroleum-based polymers.<sup>[98]</sup> These shortcomings may affect the durability and functionality of the material for various applications. Therefore, reinforcement with clay nanoparticles as fillers is one of the many ways to improve the properties of CA-based materials.

CA-organoclay nanocomposites showed improved thermal stability compared to pure cellulose diacetate polymers,<sup>[99]</sup> which could imply stability of the material at processing temperatures. Park et al.<sup>[40]</sup> reported the reinforcement of triethyl citrate-plasticized cellulose diacetate with Cloisite 30B organoclay. The plasticized cellulose diacetate and Cloisite 30B nanocomposites were processed by melt extrusion–injection molding to produce intercalated/exfoliated nanocomposites. Their results indicate

that the addition of the nanoclay increased the tensile strength and modulus of the CA-TEC polymer system. However, a higher plasticizer content (above 30 wt.%) reduced the exfoliation of the nanoclays into the polymer matrix.

Wibowo et al.<sup>[41]</sup> conducted studies on CA-TEC-clay nanocomposites and their mechanical, morphological, and thermal properties. CA-TEC-organoclay formulations were processed by extrusion followed by injection molding. The addition of 5 wt.% organoclay to the CA-TEC system resulted in improvements in heat deflection temperature (HDT) and a slight decrease in the coefficient of thermal expansion (CTE). Moreover, tensile strength and tensile modulus improved by  $\approx 38\%$  and  $33\%$ , respectively. In other studies, Pola et al.<sup>[98]</sup> produced active cellulose diacetate films through solvent casting, plasticized with oregano essential oil (OEO), and reinforced with 2.5 wt.% organophilic montmorillonite clay (MMT30B) for antifungal applications. As a result of the achievement of good dispersion of the organoclay, partial exfoliation of the polymer chains into the clay nanoplatelets was achieved, which resulted in improved thermal stability and rigidity. This was aided by the OEO plasticizer, which weakened intermolecular interactions and increased chain mobility of the polymer, allowing the penetration of CA chains into the interlamellar space of the clay. Moreover, this also reduced the oxygen permeation rate due to a more tortuous diffusion pathway, which resulted in a longer path for oxygen molecules to cross when permeating through the film.

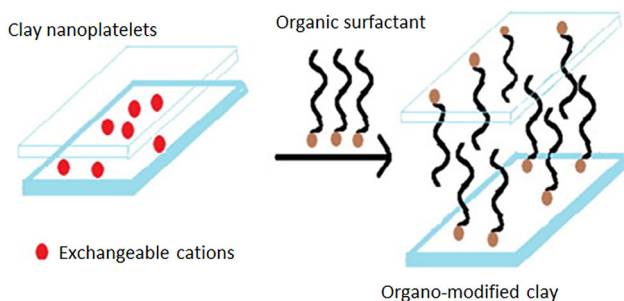
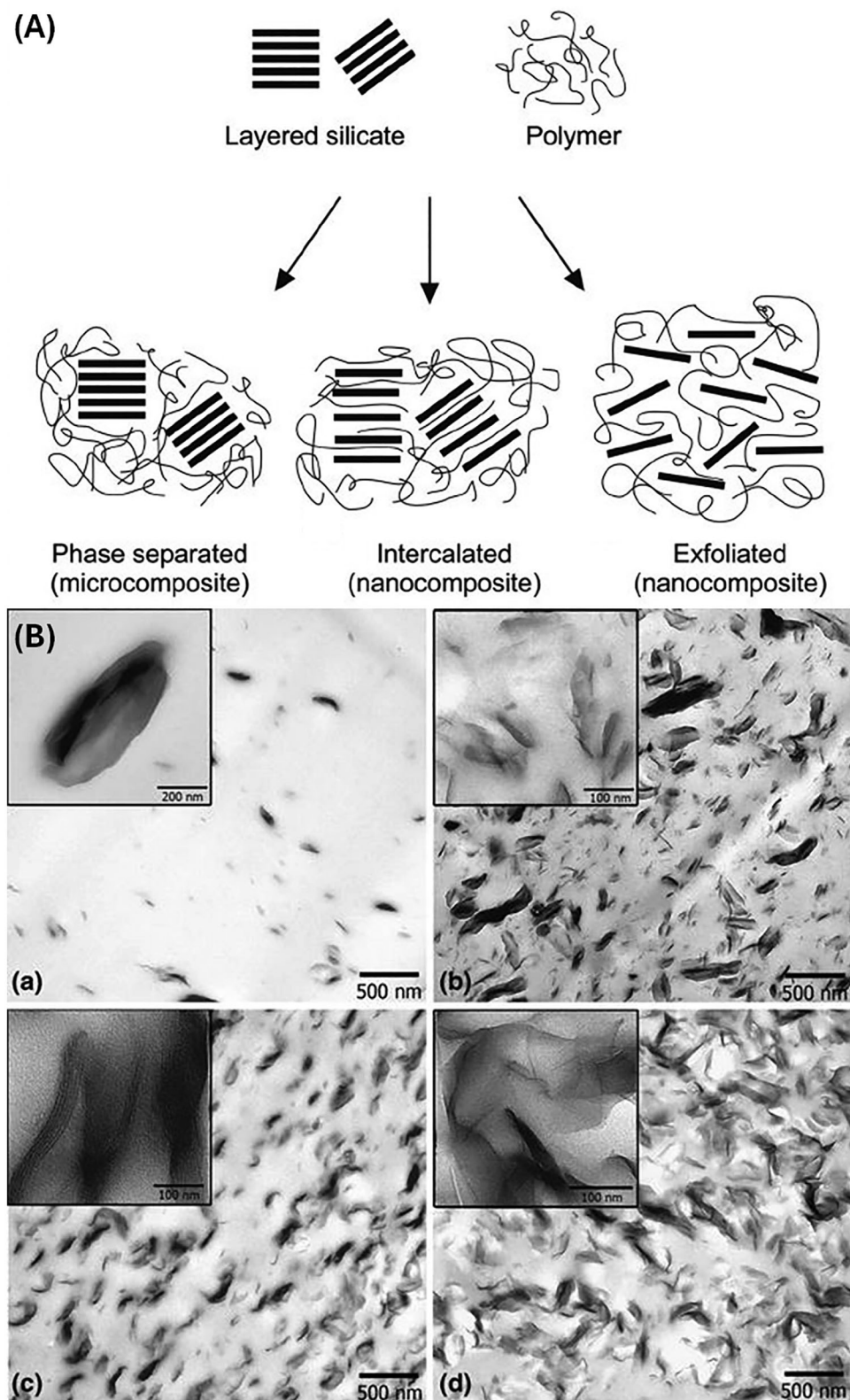


Figure 8. Schematic presentation of the modification of MMT clay with organic surfactant modifiers.<sup>[84]</sup> Reused with permission from Elsevier.

## 5. Cellulose Acetate-Based Materials in Controlled Release Technology

### 5.1. Key Principles and Kinetic Considerations of Controlled Release Technology

Controlled release is defined by Kenawy et al.<sup>[100]</sup> as a technique whereby active compounds are released to their target site at



**Figure 9.** (A) Schematic of types of micro- and nanocomposite morphologies.<sup>[79]</sup> Reused with permission from Elsevier. (B) TEM images showing the dispersion of clay nanoparticles in a CA matrix.<sup>[92]</sup> Reused with permission from Wiley.

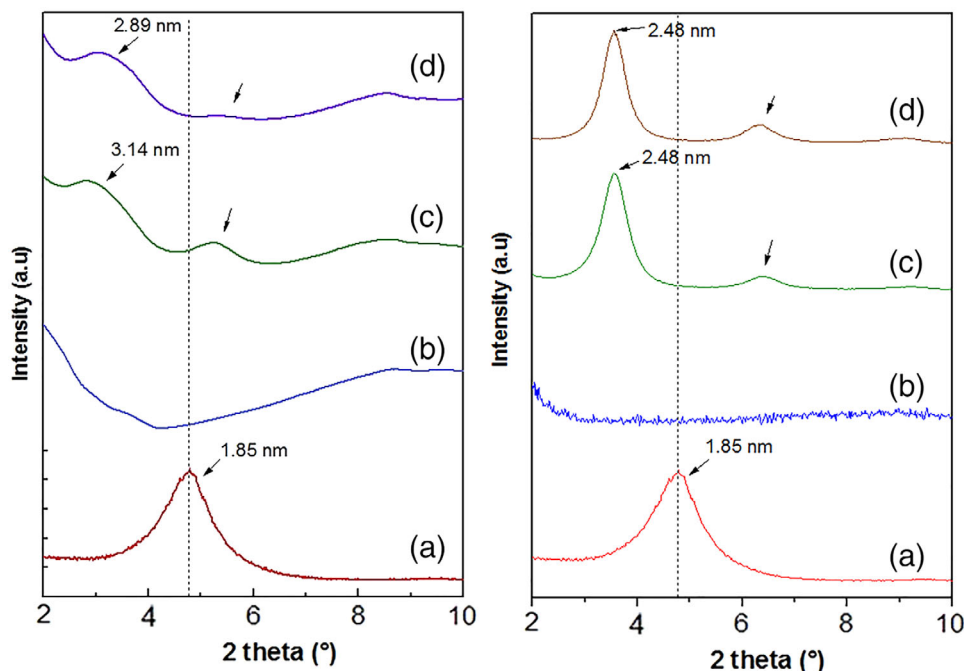


**Figure 10.** X-ray diffractograms of CA-TEC-Clay films prepared via solution casting (left) and melt processing (right). a) Cloisite 30B (C30B) clay, b) CA-TEC, c) CA-TEC-C30B; and d) CA-TEC-C30B-Cinnamaldehyde.<sup>[95]</sup> Reused with permission from Wiley.

a rate designed to accomplish the intended effect over a prolonged period. This technology is widely used in the agricultural, biomedical, and pharmaceutical industries for the objectives and advantages presented in **Figure 11**.<sup>[100–102]</sup> Importantly, controlled-release formulations should protect the active compound and release it at adequate levels above the minimum effective concentration for an extended period (**Figure 12**).<sup>[24]</sup>

Various factors affect the efficacy of controlled-release technology, which means careful consideration of materials and their properties is required for the successful fabrication of controlled-release polymeric devices.<sup>[103]</sup> The glass transition temperature ( $T_g$ ) of a polymer is one of the key factors that influence the release of active compounds from matrices. For a polymer matrix that is below its  $T_g$ , the active compound would have low diffusion rates due to the glassy state of the polymer. Above the  $T_g$ , diffusion rates would be much higher due to the rubbery state of the polymer resulting from higher chain mobility.<sup>[104]</sup> The release rate is also influenced by the following: i) Interactions between the polymer and the active compound;<sup>[100]</sup> ii) The presence of fillers, nanoparticles (e.g. clay minerals), and plasticizers; and iii) The crystallinity of the polymer matrix.<sup>[102,103]</sup> These could remarkably alter the morphology, porosity, and permeability of the resulting materials, and by extension, their ability to control the release of active compounds.<sup>[105,106]</sup> Furthermore, for an extruded cylindrical polymer strand, geometric parameters such as the strand diameter and the thickness of the outer membrane also determine the release rate of the active compound.<sup>[107]</sup>

The release of the active compounds from polymer matrices is typically governed by Fick's diffusion law, which states that the diffusion rate is dependent on dimensional factors (due to the geometry of the matrix) and diffusional factors (due to the polymer-diluent interactions).<sup>[100]</sup> Equation 4 shows the mathematical ex-

pression for the kinetics of Fick's law of diffusion at steady-state conditions.

$$R_d = \frac{dM_t}{dt} = \frac{A}{h} \cdot D (C_s - KC_e) \quad (4)$$

where  $M_t$  is the mass of the active compound released from the polymer matrix;  $R_d \propto dM_t/dt$  represents the steady-state diffusion rate of the active compound,  $A$  is the surface area through which diffusion takes place,  $h$  is the thickness of membrane through which diffusion occurs,  $D$  corresponds to the diffusion coefficient of the active compound in the polymer matrix,  $C_s$  is the solubility limit of the active compound in the polymeric membrane,  $K$  represents the partition coefficient of the active compound between the polymer and the surrounding environment, and  $C_e$  is the concentration of active compound released into the environment.

## 5.2. Cellulose Acetate-Based Materials as Controlled Release Matrices

Numerous studies have been conducted on the effectiveness of cellulose-based polymers, including cellulose acetate, as controlled-release matrices for various applications. Such materials include cellulose-based hydrogels as microcapsules and nanocapsules for encapsulating active compounds for applications such as drug delivery and agrochemicals. The absorption capabilities of superabsorbent hydrogels allow them to be used as controlled release matrices for water-soluble agrochemicals, whereby the compounds are absorbed into the matrix by swelling and slowly released by diffusion.<sup>[108]</sup> CA plays a key role as a controlled-release matrix for applications such as

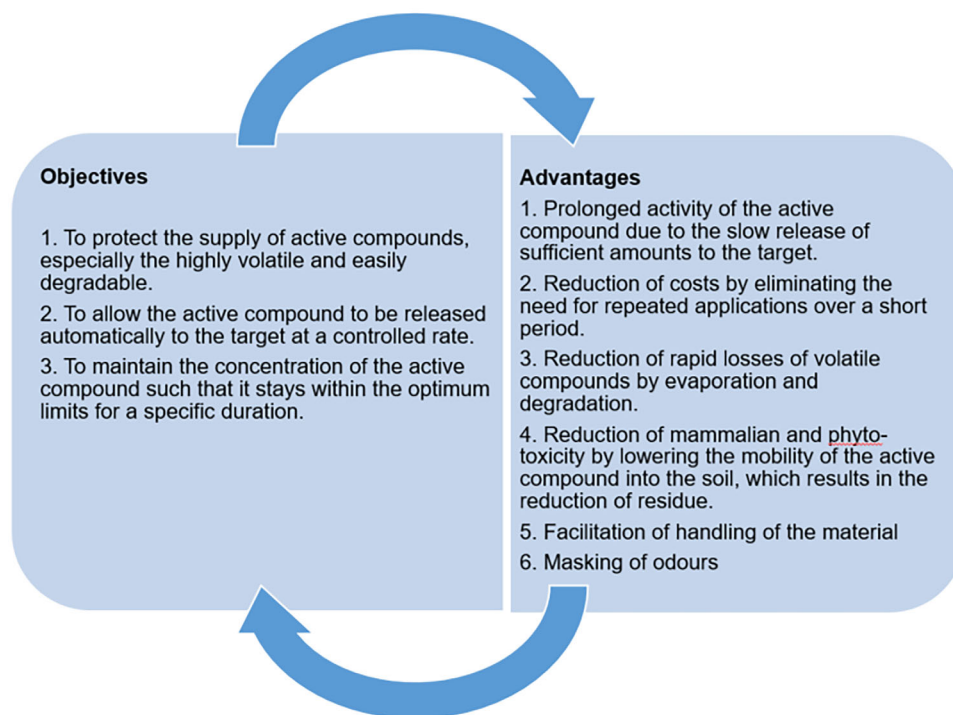


Figure 11. Objectives and advantages associated with controlled release technology.

pharmaceutical excipients, fragrances, and agricultural actives,<sup>[109]</sup> including CA beads as biocide matrices.<sup>[110]</sup>

Milovanovic et al.<sup>[109]</sup> conducted a study of cellulose acetate as a carrier for the controlled release of thymol. The authors formulated the controlled release system by means of supercritical impregnation of cellulose acetate with thymol for antibacterial applications. In their study, they report that thymol interacted with CA by hydrogen bonding, leading to the swelling of the polymer. Moreover, the amount of thymol loaded strongly affected the degree of swelling. In vitro release of thymol was studied

in solutions that resembled gastric (HCl) and intestinal (phosphate buffer, pH 7.0) fluids for at most 75 h, and release kinetics were successfully determined using the Korsmeyer-Peppas and Weibull models. Their studies showed that CA could function as a controlled-release matrix, and the release of thymol from the polymer into the surrounding solutions was mainly diffusion-mediated, with the release mechanism being affected by the type of release liquid and the amount of thymol loaded.

A study based on the development of CA-organoclay nanocomposites with citronellol, terpineol, and methyl salicylate for pest-control applications was conducted by Mphateng et al.<sup>[43]</sup> The results showed that a high quantity of active compounds (up to 35 wt.%) can be incorporated into the CA-clay matrix and released at a slow rate over at least 60 days at 40 °C (Figure 13a). This work demonstrated that extrusion-compounding is suitable for incorporating essential oils into cellulose acetate matrices for controlled-release applications. Oliviero and coworkers fabricated active packaging films consisting of triacetin-plasticized CA (DS ≈ 2.45), potassium sorbate, and a Zn(NO<sub>3</sub>)<sub>2</sub>·6H<sub>2</sub>O/Al(NO<sub>3</sub>)<sub>3</sub>·9H<sub>2</sub>O layered double hydroxide (LDH), for potential use in the food industry packaging industry. These were prepared by extrusion at a processing temperature of 160 °C. Release profiles suggested a diffusion-mediated mechanism, characterized by a slow and sustained release, attributed to the interactions between the sorbate salts and LDH particles (Figure 13b).<sup>[111]</sup>

In addition, Rodrigues Filho et al.<sup>[112]</sup> used cellulose triacetate (CTA, DS ≈ 2.8) produced from sugarcane bagasse to develop controlled-release matrices for paracetamol. The matrices were prepared by solution-casting CTA with dichloromethane and paracetamol incorporated in the initial formulations.

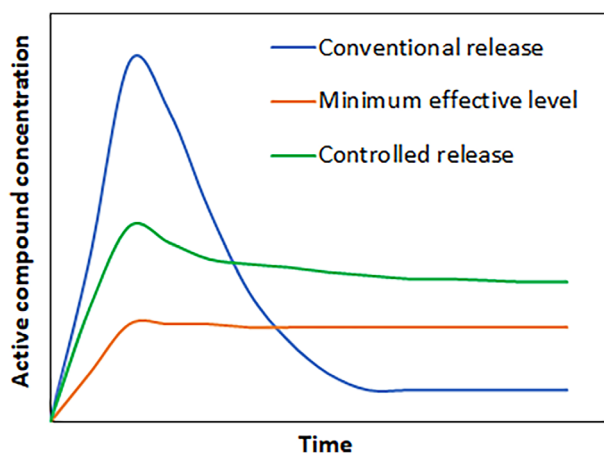
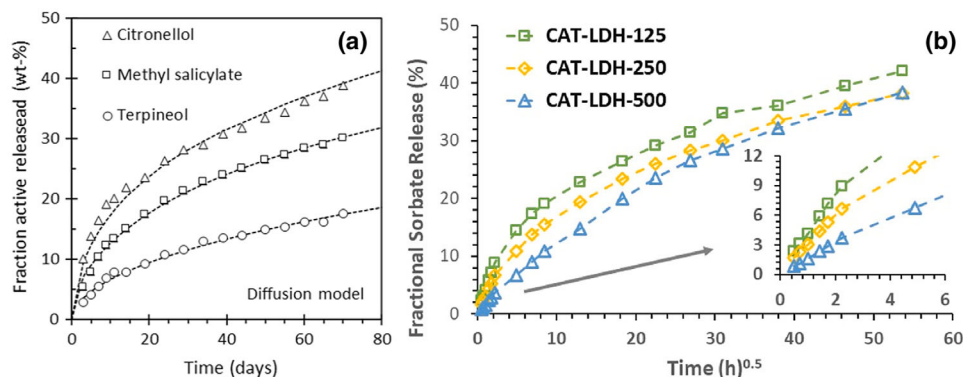


Figure 12. Differences in concentration of active compounds between conventional and controlled release formulations adapted from Roy et al.<sup>[24]</sup>



**Figure 13.** Release profiles for active compounds from CA (DS  $\approx$  2.5)-clay matrices prepared via melt extrusion. a) Citronellol, terpineol, and methyl salicylate released from CA-organoclay matrices.<sup>[43]</sup> Reproduced with permission from Springer Nature. b) Sorbate released from CA-LDH (CAT-LDH) matrices.<sup>[111]</sup> Reproduced under the CC BY 4.0 Attribution International Licence.

Moreover, water was added to the formulation (10 wt.%) to induce porosity in the films. The 8-h paracetamol release profile displayed a burst-release profile in the first 3 h, followed by a slow release thereafter. Although the active compound was not released at a controlled rate, the concept still shows good promise, and the material can be improved by incorporating nanoparticles that limit the diffusion of paracetamol in the initial stages. In another study, lysozyme was incorporated into cellulose acetate via a dry phase inversion process using a binary mixture of acetone (volatile solvent) and water (less volatile non-solvent). The cast films were then used as controlled-release matrices for lysozyme, intended for antimicrobial packaging applications. The authors reported that the release of lysozyme was diffusion-mediated and influenced by the morphology and porosity of the film, which is dependent on the composition of the CA/water/lysozyme formulation.<sup>[113]</sup>

In other studies, Pang et al.<sup>[114]</sup> prepared cellulose membranes as controlled-release matrices for biopesticides by dissolving cellulose in *N,N*-dimethylacrylamide (DMAc)/LiCl, followed by cross-linking with a dihydroxy benzophenone/Toluene diisocyanate system. Moreover, review articles by Dubey et al.,<sup>[102]</sup> Matos et al.,<sup>[110]</sup> and Roy et al.,<sup>[24]</sup> provide a detailed discussion of cellulose and its derivatives as controlled-release matrices for various active compounds.

## 6. Conclusions and Future Perspectives

Despite various studies on the development of cellulose-based materials employed in a wide array of fields, such as gas separation adsorption, filtration (nanofiltration, ultrafiltration, and microfiltration), etc., there are still few reports based on CA membranes for controlled and/or sustained release as described in this review. The principle of modification of CA membranes by incorporating clay nanoparticles to enhance their permeability, i.e., to delay the release of active compounds from CA, and overall mechanical performance was carefully described.

This review demonstrated that various studies reported in the literature are still focused on the laboratory-scale preparation and applications of CA. Regarding the fabrication of CA membranes loaded with active compounds (e.g., essential oils), rigor-

ous and extensive studies about toxicity are crucial to ensure their overall safety. Further studies on the pilot-scale development of durable CA membranes capable of releasing active agents over extended periods are important for industrial applications, including controlled-release systems.

It is also important to explore the use of active compounds from plant-based essential oils as plasticizers for CA. This concept has yielded promising results in the melt processing of CA and could potentially reduce the reliance on conventional plasticizers such as triacetin and triethyl citrate. This could be advantageous in systems where the incorporation of a conventional plasticizer could inhibit the release of active compounds from the CA matrix. Therefore, studies on the effects of conventional plasticizers on the release kinetics of active compounds are recommended, especially in cases where the active compounds are capable of functioning as plasticizers.

Due to the exigence of science and nanotechnology, more studies based on the development of cellulose acetate membranes with active ingredients and other emergent nanomaterials such as layered double hydroxides (LDH), silica may be needed and highly encouraged to add the studies already existing in the literature.

Finally, it is recommended that mathematical models that describe the mechanistic and kinetic aspects are extensively explored, including the derivation of new models for the diffusion of active agents from CA membranes. Mathematical models are important in validating experimental data and making predictions regarding the release kinetics of active agents (i.e., the time taken for an active agent to be expelled from a matrix).

## Acknowledgements

The authors express their gratitude to Emeritus Professor Walter Focke (University of Pretoria's Institute of Applied Materials, Department of Chemical Engineering) for his support. They also thank the Centre for Advanced Polymers and Nanotechnology (CAPNA), Department of Chemical and Petroleum Engineering, University of Calgary, Canada for their support. This work was financially supported by the Paper Manufacturers Association of South Africa (PAMSA) and the Department of Science and Innovation (DSI) under Grant DST/CON 0004/2019, and the National Research Foundation of South Africa (NRF) (Grant No.130591).

## Conflict of Interest

The authors declare no conflict of interest.

## Author Contributions

T.N.M. contributed to the conceptualization, investigation, methodology, original draft preparation, formal analysis, review and editing of the manuscript, and validation of the findings. A.B.M. contributed to the investigation, original draft preparation, review and editing of the manuscript, and validation of the findings. T.M. contributed to the investigation, original draft preparation, review and editing of the manuscript, and validation of the findings. S.S.R. contributed to the review and editing of the manuscript, formal analysis, and validation of the findings. U.S. contributed to the review and editing of the manuscript, formal analysis, and validation of the findings.

## Keywords

cellulose acetate, controlled release, encapsulation technology, melt processing

Received: March 14, 2025

Revised: April 13, 2025

Published online:

- [1] R. Konwarh, N. Karak, M. Misra, *Biotechnol. Adv.* **2013**, *31*, 421.
- [2] A. Okhovat, F. Z. Ashtiani, M. Karimi, *J. Polym. Res.* **2015**, *22*, 234.
- [3] V. T. Phuong, S. Verstiche, P. Cinelli, I. Anguillesi, M.-B. Coltelli, A. Lazzeri, *J. Renew. Mater.* **2014**, *2*, 35.
- [4] P. Fei, L. Liao, B. Cheng, J. Song, *Anal. Methods* **2017**, *9*, 6194.
- [5] C. Bao, *PhD Thesis, Université Claude Bernard Lyon 1, Villeurbanne* **2015**.
- [6] M. A. Wsoo, S. Shahir, S. P. Mohd Bohari, N. H. M. Nayan, S. I. A. Razak, *Carbohydr. Res.* **2020**, *491*, 107978.
- [7] R. Quintana, O. Persenaire, L. Bonnaud, P. Dubois, *Polym. Chem.* **2012**, *3*, 591.
- [8] R. Quintana, O. Persenaire, Y. Lemmouchi, J. Sampson, S. Martin, L. Bonnaud, P. Dubois, *Polym. Degrad. Stab.* **2013**, *98*, 1556.
- [9] B. Han, D. Zhang, Z. Shao, L. Kong, S. Lv, *Desalination* **2013**, *311*, 80.
- [10] S. Zepnik, S. Kabasci, R. Kopitzky, H.-J. Radosch, T. Wodke, *Polymers* **2013**, *5*, 873.
- [11] A. Bendaoud, Y. Chalamet, *Carbohydr. Polym.* **2014**, *108*, 75.
- [12] S. Ramesh, R. Shanti, E. Morris, *Carbohydr. Polym.* **2013**, *91*, 14.
- [13] S. Ramesh, R. Shanti, E. Morris, *Cellulose* **2013**, *20*, 1377.
- [14] D. Rui, M. Li, *Expert Rev. Chinese Chem.* **2024**, *2*, 32.
- [15] J. Puls, S. A. Wilson, D. Hölter, *J. Polym. Environ.* **2010**, *19*, 152.
- [16] L. S. F. Leite, L. C. Battirola, L. C. E. da Silva, M. d. C. Gonçalves, *J. Appl. Polym. Sci.* **2016**, *133*, 105.
- [17] C. Brigham, in *Green Chemistry* (Eds.: B. Török, T. Dransfield), Elsevier, Netherlands **2018**, pp. 753.
- [18] Y. Teramoto, *Molecules* **2015**, *20*, 5487.
- [19] H. Wang, G. Gurau, R. D. Rogers, *Chem. Soc. Rev.* **2012**, *41*, 1519.
- [20] M. S. Gilbert, I. Palle, in *Int. Proc. of Chemical, Biological and Environmental Engineering*, IACSIT Press, Singapore, **2013**, Vol. 58, pp. 115.
- [21] S. Zepnik, S. Kabasci, R. Kopitzky, H.-J. Radosch, T. Wodke, *Polymers* **2013**, *5*, 873.
- [22] S. Zepnik, T. Hildebrand, S. Kabasci, H.-J. Radosch, T. Wodke, in *Cellulose: Biomass Conversion* (Ed.: J. Kadla, T. van de Ven), InTech, Rijeka **2013**.
- [23] X. Dreux, J. C. Majeste, C. Carrot, A. Argoud, C. Vergelati, *Carbohydr. Polym.* **2019**, *222*, 114973.
- [24] A. Roy, S. K. Singh, J. Bajpai, A. K. Bajpai, *Cent. Eur. J. Chem.* **2014**, *12*, 453.
- [25] N. S. Allen, M. Edge, J. H. Appleyard, T. S. Jewitt, *Polym. Degrad. Stab.* **1987**, *19*, 379.
- [26] R. Xu, C. Yin, J. Zhang, Y. Zhou, Q. Mi, J. Zhang, *ACS Sustain. Chem. Eng.* **2022**, *10*, 2822.
- [27] F. Shen, D. Tian, G. Yang, S. Deng, F. Shen, J. He, Y. Zhu, C. Huang, J. Hu, *ACS Sustain. Chem. Eng.* **2020**, *8*, 11253.
- [28] C. M. Buchanan, R. M. Gardner, R. J. Komarek, *J. Appl. Polym. Sci.* **1993**, *47*, 1709.
- [29] M. Y. Arancibia, M. E. López-Caballero, M. C. Gómez-Guillén, P. Montero, *Food Control* **2014**, *44*, 7.
- [30] D. Beaton, P. Pelletier, R. Goulet, *Front. Microbiol.* **2019**, *10*.
- [31] B. M. Tselana, S. Muniyasamy, V. O. Ojijo, W. Mhike, *J. Polym. Environ.* **2023**, *31*, 4891.
- [32] C. M. Buchanan, D. Dorschel, R. M. Gardner, R. J. Komarek, A. J. Matosky, A. W. White, M. D. Wood, *J. Environ. Polym. Degrad.* **1996**, *4*, 179.
- [33] F. Degli-Innocenti, M. Tosin, C. Bastioli, *J. Environ. Polym. Degrad.* **1998**, *6*, 197.
- [34] S. Verstichel, B. De Wilde, E. Fenyvesi, J. Szejtli, *J. Polym. Environ.* **2004**, *12*, 47.
- [35] K. Hosono, A. Kanazawa, H. Mori, T. Endo, *J. Appl. Polym. Sci.* **2007**, *105*, 3235.
- [36] K. Kamide, M. Saito, *Polym. J.* **1985**, *17*, 919.
- [37] C. Hopmann, C. Windeck, S. Hendriks, S. Zepnik, T. Wodke, **2014**, *AIP Conf. Proc.* **1593**, 116.
- [38] A. Charvet, C. Vergelati, D. R. Long, *Carbohydr. Polym.* **2019**, *204*, 182.
- [39] C. Decroix, Y. Chalamet, G. Sudre, V. Caroll, *Carbohydr. Polym.* **2020**, *237*, 116072.
- [40] H. M. Park, M. Misra, L. T. Drzal, A. K. Mohanty, *Biomacromolecules* **2004**, *5*, 2281.
- [41] A. C. Wibowo, M. Misra, H.-M. Park, L. T. Drzal, R. Schalek, A. K. Mohanty, *Compos. A: Appl. Sci. Manuf.* **2006**, *37*, 1428.
- [42] C. Y. Bao, D. R. Long, C. Vergelati, *Carbohydr. Polym.* **2015**, *116*, 95.
- [43] T. N. Mphateng, A. B. Mapossa, J. Wesley-Smith, S. Ramjee, W. W. Focke, *Cellulose* **2022**, *29*, 3915.
- [44] C. R. Fordyce, I. W. A. Meyer, *Ind. Eng. Chem.* **1940**, *32*, 1053.
- [45] R. Erdmann, S. Kabasci, H. P. Heim, *Polymers (Basel)* **2021**, *13*, 1356.
- [46] A. Bonifacio, L. Bonetti, E. Piantanida, L. De Nardo, *Eur. Polym. J.* **2023**, *197*, 112360.
- [47] G. Tedeschi, S. Guzman-Puyol, U. C. Paul, M. J. Barthel, L. Goldoni, G. Caputo, L. Ceseracci, A. Athanassiou, J. A. Heredia-Guerrero, *Chem. Eng. J.* **2018**, *348*, 840.
- [48] A. Delgado-Lima, M. Paiva, A. Machado, *J. Renew. Mater.* **2017**, *5*, 145.
- [49] C. Herniou-Julien, J. R. Mendieta, T. J. Gutiérrez, *Food Hydrocol.* **2019**, *89*, 67.
- [50] J. H. Hildebrand, R. L. Scott, *The Solubility of Nonelectrolytes*, Reinhold Pub. Corp, New York **1950**.
- [51] M. J. Louwerse, A. Maldonado, S. Rousseau, C. Moreau-Masselon, B. Roux, G. Rothenberg, *ChemPhysChem* **2017**, *18*, 2999.
- [52] M. A. Rasool, I. F. J. Vankelecom, *Green Chem.* **2019**, *21*, 1054.
- [53] S. Scheler, A. Fahr, X. Liu, *Admet & Dmpk* **2015**, *2*, 199.
- [54] G. Wypych, *Handbook of Solvents, 1*, ChemTec Publishing, Canada **2019**.
- [55] M. T. Garcia, I. Gracia, G. Duque, A. Lucas, J. F. Rodriguez, *Waste Manag.* **2009**, *29*, 1814.
- [56] B. Ghorani, S. J. Russell, P. Goswami, *Int. J. Polym. Sci.* **2013**, *2013*, 1.

- [57] M. Batista, R. Guirardello, M. Kraehenbuehl, *J. Am. Oil Chem. Soc.* **2015**, 92, 95.
- [58] S. I. Swapnil, N. Datta, M. M. Mahmud, R. A. Jahan, M. T. Arafat, *J. Appl. Polym. Sci.* **2020**, 138, 50358.
- [59] S. Majumder, M. A. Matin, A. Sharif, M. T. Arafat, *Bull. Mater. Sci.* **2019**, 42, 171.
- [60] J. Burke, *Solubility Parameters: Theory and Application*, <https://cool.conservation-us.org/coolaic/sg/bpg/annual/v03/bp03-04.html>, **1984**, 3.
- [61] X. Zhang, L. Yang, C. Zhang, D. Liu, S. Meng, W. Zhang, S. Meng, *Pharmaceutics* **2019**, 11, 520.
- [62] B. Liu, Q. Du, Y. Yang, *J. Membrane Sci.* **2000**, 180, 81.
- [63] M. H. Alqarni, N. Haq, P. Alam, M. S. Abdel-Kader, A. I. Foudah, F. Shakeel, *J. Mol. Liq.* **2021**, 331, 115700.
- [64] H. Yamamoto, Hansen Solubility Parameters (HSP) Application Notes, <https://pirika.com/NewHP/PirikaE/Flavor.html>, **2013**.
- [65] S. Abbot, *HSP Basics*, <https://www.stevenabbott.co.uk/practicalsolubility/hsp-basics.php> **2019**.
- [66] C. M. Hansen, *Hansen Solubility Parameters: A User's Handbook*, 2nd ed., CRC Press, Boca Raton, **2007**.
- [67] R. Muthuraj, M. Misra, A. K. Mohanty, *J. Appl. Polym. Sci.* **2017**, 135, 45726.
- [68] P. Couchman, *Macromolecules* **1978**, 11, 1156.
- [69] J. H. Kim, J. Jang, D.-Y. Lee, W.-C. Zin, *Macromolecules* **2002**, 35, 311.
- [70] T. G. Fox, *Bull. Am. Phys. Soc.* **1956**, 1, 123.
- [71] E. Jenckel, R. Heusch, *Kolloid-Zeitschrift* **1953**, 130, 89.
- [72] P. R. Couchman, F. E. Karasz, *Macromolecules* **1978**, 11, 117.
- [73] M. Gordon, J. S. Taylor, *J. Appl. Chem.* **1952**, 2, 493.
- [74] W. W. Young, J. P. Saez, R. Katsumata, *ACS Macro Lett.* **2021**, 10, 1404.
- [75] J. Parameswaranpillai, S. Thomas, Y. Grohens, *Characterization of Polymer Blends*, Wiley, New Jersey, **2014**, 1.
- [76] A. R. Fialho e Moraes, C. C. Pola, A. P. Bilck, F. Yamashita, J. Tronto, E. A. A. Medeiros, N. d. F. F. Soares, *Mater. Sci. Eng.: C* **2017**, 78, 932.
- [77] K. W. Meereboer, A. K. Pal, M. Misra, A. K. Mohanty, *ACS Omega* **2020**, 5, 14221.
- [78] C. S. Marques, R. R. Silva, T. R. Arruda, A. L. Ferreira, T. V. Oliveira, A. R. Moraes, M. V. Dias, M. C. Vanetti, N. D. Soares, *Polysaccharides* **2022**, 3, 277.
- [79] M. Alexandre, P. Dubois, *Mater. Sci. Eng.* **2000**, 28, 1.
- [80] T. V. Duncan, *J. Colloid Interface Sci.* **2011**, 363, 1.
- [81] M. K. M. Haafiz, A. Hassan, H. P. S. A. Khalil, M. R. N. Fazita, M. S. Islam, I. M. Inuwa, M. M. Marliana, M. H. Hussin, *Int. J. Biol. Macromol.* **2016**, 85, 370.
- [82] J. George, S. N. Sabapathi, *Nanotechnol. Sci. Appl.* **2015**, 8, 45.
- [83] Y. Cui, S. Kumar, B. Rao Kona, D. van Houcke, *RSC Adv.* **2015**, 5, 63669.
- [84] K. Majeed, M. Jawaid, A. Hassan, A. A. Bakar, H. P. S. Abdul Khalil, A. A. Salema, I. Inuwa, *Mater. Des.* **2013**, 46, 391.
- [85] H. Salam, Y. Dong, I. Davies, in *Fillers and Reinforcements for Advanced Nanocomposites* (Eds.: Y. Dong, R. Umer, A. K.-T. Lau), Woodhead Publishing, Cambridge, **2015**, pp. 101.
- [86] Q. Duan, S. Jiang, F. Chen, Z. Li, L. Ma, Y. Song, X. Yu, Y. Chen, H. Liu, L. Yu, *Ind. Crop. Prod.* **2023**, 192, 116075.
- [87] F. J. Rodríguez, M. J. Galotto, A. Guarda, J. E. Bruna, *J. Food Eng.* **2012**, 110, 262.
- [88] M. Hassan-Nejad, J. Ganster, A. Bohn, M. Pinnow, B. Volkert, *Macromol. Symp.* **2009**, 280, 123.
- [89] H. Ferfera-Harrar, N. Dairi, *Iran. Polym. J.* **2014**, 23, 917.
- [90] S. S. Ray, M. Okamoto, *Prog. Polym. Sci.* **2003**, 28, 1539.
- [91] H. M. C. de Azeredo, L. H. C. Mattoso, T. H. McHugh, in *Advances in Diverse Industrial Applications of Nanocomposites* (Ed.: B. S. R. Reddy), InTech, Rijeka **2011**, p. 57.
- [92] R. B. Romero, M. M. F. Ferrarezi, C. A. P. Leite, R. M. V. Alves, M. d. C. Gonçalves, *Cellulose* **2012**, 20, 675.
- [93] B. Nkonki-Mandleni, F. T. Ogunkoya, A. O. Omotayo, *Int. J. Entrep.* **2019**, 23, 1.
- [94] J. A. de Lima, C. Augusto Pinotti, M. I. Felisberti, M. do Carmo Gonçalves, *J. Appl. Polym. Sci.* **2011**, 124, 4628.
- [95] F. J. Rodríguez, R. L. Abarca, J. E. Bruna, P. E. Moya, M. J. Galotto, A. Guarda, M. Padula, *Polym. Comp.* **2018**, 40, 2311.
- [96] M. D. Raicopol, C. Andronescu, S. I. Voicu, E. Vasile, A. M. Pandeale, *Carbohydr. Polym.* **2019**, 214, 204.
- [97] G. Arthanareeswaran, P. Thanikaivelan, K. Srinivasn, D. Mohan, M. Rajendran, *Eur. Polym. J.* **2004**, 40, 2153.
- [98] C. C. Pola, E. A. A. Medeiros, O. L. Pereira, V. G. L. Souza, C. G. Otoni, G. P. Camilloto, N. F. F. Soares, *Food Packag. Shelf Life* **2016**, 9, 69.
- [99] H. Ferfera-Harrar, N. Dairi, *Polym. Compos.* **2013**, 34, 1515.
- [100] E. R. Kenawy, D. C. Sherrington, A. Akelah, *Eur. Polym. J.* **1992**, 28, 841.
- [101] A. Akelah, *Mater. Sci. Eng.: C* **1996**, 4, 83.
- [102] S. Dubey, V. Jhelum, P. K. Patanjali, *J. Sci. Ind. Res.* **2011**, 70, 105.
- [103] R. W. Korsmeyer, N. A. Peppas, *J. Membr. Sci.* **1981**, 9, 211.
- [104] F. Pilati, M. Degli Esposti, M. Bondi, R. Iseppi, M. Toselli, *J. Mater. Sci.* **2013**, 48, 4378.
- [105] Y.-J. Wang, Z.-P. Zhao, Z.-Y. Xi, S.-Y. Yan, *J. Membrane Sci.* **2018**, 548, 332.
- [106] S. Kim, Y. M. Lee, *Prog. Polym. Sci.* **2015**, 43, 1.
- [107] A. B. Mapossa, M. M. Sibanda, A. Siteo, W. W. Focke, L. Braack, C. Ndongyane, J. Mouatcho, J. Smart, H. Muaimbo, R. Androsch, M. T. Loots, *Chem. Eng. J.* **2019**, 360, 435.
- [108] L. Pang, Z. Gao, H. Feng, S. Wang, Q. Wang, *J. Controlled Release* **2019**, 316, 105.
- [109] S. Milovanovic, D. Markovic, K. Aksentijevic, D. B. Stojanovic, J. Ivanovic, I. Zizovic, *Carbohydr. Polym.* **2016**, 147, 344.
- [110] B. D. Mattos, B. L. Tardy, W. L. E. Magalhaes, O. J. Rojas, *J. Control Release* **2017**, 262, 139.
- [111] M. Oliviero, E. Lamberti, L. Cafiero, B. Pace, M. Cefola, G. Gorrasi, A. Sambandam, A. Sorrentino, *Mater. Chem. Phys.* **2023**, 310, 128469.
- [112] G. Rodrigues Filho, F. Almeida, S. D. Ribeiro, T. F. Tormin, R. A. Munoz, R. M. Assuncao, H. Barud, *Drug Dev. Ind. Pharm.* **2016**, 42, 1066.
- [113] S. Gemili, A. Yemenicioğlu, S. A. Altinkaya, *J. Food Eng.* **2009**, 90, 453.
- [114] L. Pang, Z. Gao, S. Zhang, Y. Li, S. Hu, X. Ren, *Ind. Crop. Prod.* **2016**, 89, 176.



**Thabang N. Mphateng** obtained his M.Sc. from the University of Pretoria (South Africa), where his research focused on cellulose-based materials for controlled release applications. He then obtained a Ph.D. in Polymer Science from Stellenbosch University (South Africa), where he is currently a post-doctoral fellow. His research interests are in the development of advanced polymer-based materials for multifunctional applications, including controlled release matrices for various active compounds, adsorbents for wastewater remediation, and tissue engineering scaffolds.



**António Benjamim Mapossa** obtained a Ph.D. from the Department of Chemical Engineering at the University of Pretoria, South Africa, where he also began working as a postdoctoral researcher. Currently, he is a Research Associate in the Department of Chemical and Petroleum Engineering at the University of Calgary, Canada. His research primarily focuses on Materials Science and Engineering, specifically examining the structure, processing, and properties of polymer nanocomposites and non-magnetic materials for applications in malaria, agriculture, flooring materials, biodiesel, and water and wastewater treatment. He is a Y2-NRF-rated researcher with a strong record of research productivity and high-quality research evaluated and benchmarked by the South African National Research Foundation, recognized by peers in his field.



**Teboho C. Mokhena** obtained a Ph.D. degree in Polymer Science at the University of the Free State, South Africa in 2017. He is working as a Principal Research Scientist at MINTEK Advanced Materials Division. His research focuses on the exploitation of waste materials to fabricate value added nanostructured materials for advanced applications.



**Suprakas Sinha Ray** is the chief researcher and director of DST/CSIR National Centre for Nanostructured Materials, CSIR, South Africa, and an Extraordinary Professor at the University of Johannesburg, South Africa. He is one of the most active and highly cited authors in the field of polymer nanocomposite materials, and recently, he has been rated as one of the top 50 high-impact chemists in the world (Feb. 2011, Thomson Reuter).



**Uttandaraman Sundararaj** joined the University of Calgary in August 2009. Previously, he was a Professor at the University of Alberta for 12 years. He has 4 years of industrial experience with General Electric Company - Plastics Division. He was a visiting Professor at the University of California - Santa Barbara, University of Paderborn (Germany), Institute for Polymer Research - Dresden (Germany), and at Dupont Experimental Station - Delaware.